Published in final edited form as:
Exp Neurol. 2014 November ; 0: 65–75. doi:10.1016/j.expneurol.2014.06.013.

Expression of Suppressor of Cytokine Signaling-3 (SOCS3) and its role in neuronal death after complete spinal cord injury

Keun Woo Park, **Ching-Yi Lin**, and **Yu-Shang Lee***
Department of Neurosciences, Lerner Research Institute, Cleveland Clinic, Cleveland, Ohio 44195

Abstract

The present study investigates the endogenous expression of Suppressor of Cytokine Signaling-3 (SOCS3) after spinal cord injury (SCI) and its effect on SCI-induced cell death *in vivo*. In addition, we determined whether a reduction of SOCS3 expression induced by microinjection of short hairpin RNA (shSOCS3) carried by lentivirus into spinal cord provides cellular protection after SCI. We demonstrated that complete transection of rat T8 spinal cord induced SOCS3 expression at the mRNA and protein levels as early as 2 days post-injury, which was maintained up to 14 days. SOCS3 immunoreactivity was detected in neurons and activated microglia after SCI. We also demonstrated that SCI induces phosphorylation of proteins that are involved in signal transduction and transcription-3 (STAT3) in neurons, which induced SOCS3 expression. Western blot analyses and double-immunofluorescent staining showed significant up-regulation of the pro-apoptotic protein Bax, increases in the ratio of Bax to the anti-apoptotic protein Bcl-2, and up-regulation of cleaved caspase-3 in neurons. Treatment with shSOCS3 inhibited SCI-induced mRNA expression of SOCS3 2 days post-injury and suppressed SCI-induced Bax expression 7 days after SCI, both rostral and caudal to the lesion. Moreover, treatment with shSOCS3 inhibited SCI-induced neuronal death and protected neuronal morphology both rostral and caudal to the injury site 7 days post-injury. Our results suggest that the STAT3/SOCS3 signaling pathway plays an important role in regulating neuronal death after SCI.

Keywords

Suppressor of Cytokine Signaling-3; neuronal death; short hairpin RNA; Bax/Bcl-2; neuroplasticity; spinal cord injury

*Address for correspondence: Send correspondence to: Yu-Shang Lee, Ph.D., Department of Neurosciences, Cleveland Clinic, 9500 Euclid Avenue / NC30, Cleveland, OH 44195: leey2@ccf.org; Telephone: (216) 445-5040; Fax: (216) 636-4332.

INTRODUCTION

Spinal cord injury (SCI) initiates a series of cellular and molecular events that include direct mechanical damage and subsequent secondary injury cascades (Beattie et al., 2002; Beattie, 2004). Direct mechanical damage induces a cascade of excitotoxicity, oxidative stress, and membrane breakdown. This in turn triggers secondary injury cascades, including glia activation and inflammatory cytokine expression, which lead to secondary cell death of neurons and glia (Hausmann, 2003; Lu et al., 2000). Several reports have demonstrated that complete SCI, resulting in apoptotic neuronal death, is characterized by chromatin condensation, DNA fragmentation, and pro-apoptotic Bax expression *in vivo* (Stirling et al., 2004; Wu et al., 2007). The main regulators of apoptotic cell death are members of the Bcl-2 family, which include Bax and anti-apoptotic Bcl-2 (Ola et al., 2011; Rahman et al., 2012). Bax forms heterodimers with Bcl-2 and the ratio of Bax/Bcl-2 modulates mitochondrial outer membrane permeability (Oltvai et al., 1993). This is central to the regulation of caspase-dependent apoptotic cell death (Tsujimoto, 2003).

Additionally, Suppressor of Cytokine Signaling (SOCS) proteins have been shown to play a role in terminating signaling through the JAK/STAT pathway (Yoshimura et al., 2007; Baker et al., 2009) that regulates neuronal growth and differentiation. SOCS3 expression in neurons in particular caused a negative regulatory effect on signal transduction and transcription-3 (STAT3) activation, which consequently contributed to excitotoxic neuronal death *in vitro* (Park et al., 2012). The inhibition of neuronal protection by SOCS3 was shown to act through anti-apoptotic Bcl-xL, indicating a deleterious effect of SOCS3 on neuronal survival. SOCS3 binds to gp130, a common signal transducing subunit with interleukin-6 (IL-6), or to Janus kinase1 (JAK1) and JAK2, to inhibit signal transduction (Nicholson et al., 2000; Schmitz et al., 2000). This results in negative regulation of neuronal survival and axon regeneration (Yadav et al., 2005; Miao et al., 2008; Sun et al., 2011) *in vivo* and *in vitro*. These studies demonstrated that SOCS3 expression negatively regulates phosphorylation of STAT3, leading to inhibition of neuronal protection and axonal regeneration. However, the levels and pattern of SOCS3 expression in the spinal cord and how SOCS3 contributes to cell death regulation after SCI *in vivo* are currently unknown.

Here, we hypothesize that up-regulation of SOCS3 can lead to cell death after SCI by complete transection (Tx) of the T8 spinal cord and that inhibition of SCI-induced SOCS3 expression in neurons can provide neuroprotective effects. We determined the expression pattern of SOCS3 in different cell types and at different time points and analyzed correlation with cell death after complete SCI in adult rats. We also investigated the underlying mechanism of SOCS3-mediated apoptotic cell death, including its interactions with Bcl-2, Bax, and caspase-3. Finally, we demonstrated that the survival rate of neurons after SCI was enhanced when SCI-induced SOCS3 expression was reduced by microinjection of short hairpin RNA specific for SOCS3 (shSOCS3) into the spinal cord.

MATERIALS AND METHODS

Animals

One hundred and four adult female Sprague-Dawley rats (220–250g) were assigned randomly into six groups: (1) sham control group (laminectomy only; n=13); (2) Tx-only group (T8 spinal cord transection only; n=49); (3) sham + control lentivirus (pGipz) group (laminectomy only with pGipz injection; n=9); (4) Tx + pGpiz group (T8 spinal cord transection with pGipz injection; n=12); (5) sham + lentivirus carrying shSOCS3 (shSOCS3) group (laminectomy only and shSOCS3 injection; n=9); (6) Tx + shSOCS3 group (T8 spinal cord transection and shSOCS3 injection; n=12). Rats were housed in standard laboratory cages with a 12:12 hour light/dark cycle with standard rodent chow and water available *ad libitum*. The experiments were performed during the light cycle. All animal procedures were approved by the Cleveland Clinic Institutional Animal Care and Use Committee (IACUC).

Spinal cord surgery and delivery of shSOCS3 to the spinal cord

All surgical procedures were conducted under aseptic conditions. Before surgery, all animals were anesthetized with 2% isoflurane gas mixed with oxygen. Rats were maintained on a heating pad and rectal temperature was monitored and maintained within ± 1.5°C of 36.5°C during surgery. Animals in the sham control group underwent a laminectomy only (T8 level). In the Tx-only group, a laminectomy was also performed, followed by complete transverse cuts of the spinal cord at the T8 level, resulting in a gap of ~2–3 mm. A surgical microscope was used to ensure the complete removal of neural tissue, including fiber bundles. Muscle and skin layers were closed with 2-0 sutures. The bladders of all spinal cord-transected rats were expressed manually twice per day throughout the experimental period.

A lentiviral plasmid encoding shRNA specific for SOCS3 to knock down SOCS3 expression, shSOCS3/pGpiz, was obtained from Dr. Etty Benveniste (University of Alabama at Birmingham). Briefly, as previously described (Park et al., 2012), lentiviral particles were generated by calcium phosphate-mediated co-transfection of HEK-293T cells with empty pGipz or shSOCS3/pGpiz, psPAX2 (Packaging plasmid), and pMD2G (Envelope plasmid). Virus was collected after 72 h and titers up to $3–4\times10^9$ infectious units/ml were obtained.

For lentiviral injections into the spinal cord, a laminectomy was performed at T8, followed by insertion of a pored glass pipette attached to a microinjector into the gray matter of the spinal cord. The target areas for injection included four total sites at the following coordinates: two sites 2.5 mm rostral and two sites 2.5 mm caudal to the injury site; depth was 2 mm below the spinal cord at each site. Infusions were made at a rate of 133nl /min for pGipz or shSOCS3 containing lentivirus (2×10^7 total infectious units in 4 μl). After injection, the glass pipette was left in place for an additional 2 min before being slowly retracted. In the sham + pGipz group, Tx + pGipz group, sham + shSOCS3 group, and Tx + shSOCS3 group, lentiviral delivery into the spinal cord was performed 2 weeks before the T8 spinal cord transection or sham procedure.

Immunohistochemistry

Animals were anesthetized at the indicated time points (1, 2, 4, 7 or 14 days) after SCI and transcardially perfused with 0.9% saline followed by 4% paraformaldehyde. Spinal cord tissues were removed, post-fixed overnight at 4 °C in buffered 4% paraformaldehyde, and stored at 4 °C in 30% sucrose solution until sinking. The tissues were then transversely sectioned (30 μm) and collected using a cryostat. Immunohistochemistry was performed as described previously (Lee et al., 2013). Briefly, free-floating serial sections were rinsed three times for 10 min with PBS and blocked with PBS containing 3% normal horse serum and 0.25% Triton X-100 for 1 h at room temperature. After blocking, the sections were incubated overnight with gentle agitation at room temperature with PBS containing 0.5% BSA in the following antibody combinations: the neuronal-specific nuclear protein NeuN (1:5000; EMD Millipore, Billerica, MA) for neurons with SOCS3 (1:1,000; abcam, Cambridge, MA), glial fibrillary acidic protein (GFAP) for astrocytes (1:4,000; Dako, Glostrup, Denmark) with SOCS3, OX-42 (1:1,000; Thermo Scientific, Rockford, IL), which recognizes complement receptor 3, with SOCS3, NeuN with phosphorylated STAT3 Tyr 705 (1:1,000; Cell Signaling Technology, Beverly, MA), or NeuN with cleaved caspase-3 (1:1,000; Cell Signaling Technology). Sections were then rinsed in PBS and incubated for 1 h at room temperature with the secondary antibody conjugated by Alexa Flour 488 or 594 as appropriate (1:2,000; Life Technologies, Grand Island, NY). Tissues were then washed and mounted with Vectashield mounting medium (Vector Laboratory, Burlingame, CA). Sections were examined and all images were taken using a fluorescent microscope (DM6000; Leica Microsystems, Buffalo Grove, IL).

TUNEL staining

The amount of apoptosis was determined by double-staining of TUNEL with NeuN, GFAP, or OX-42. TUNEL assays were performed using the Apoptag fluorescein *in situ* detection kit (Roche Applied Science, Indianapolis, IN) that detects the 3′-OH region of cleaved DNA during apoptosis. Briefly, sections of spinal cord tissue were permeabilized with 3% normal horse serum with 0.25% Triton X-100 in PBS for 30 min at room temperature. The TUNEL reaction mixture was then added; tissue was incubated in a humidified chamber for 1 h at 37°C and washed with PBS. For double staining, sections were incubated with antibody against NeuN, GFAP, or OX-42 overnight at room temperature. The next day, sections were rinsed with PBS and incubated for 1 h at room temperature with Alexa Flour 594-conjugated secondary antibody (Life Technologies). Tissues were then washed and mounted with Vectashield mounting medium (Vector Laboratory). Images were collected using a fluorescent microscope (DM6000; Leica Microsystems).

Western blotting

Spinal cord tissues were obtained from areas 5 mm rostral and caudal to the epicenter and were homogenized in ice-cold lysis buffer containing the following (in mM): 20 mM Tris-HCl (pH 7.5), 1 mM EDTA, 5 mM MgCl2, 1 mM DTT, protease inhibitor mixture (Roche Applied Science) and phosphatase inhibitor I & II (Sigma-Aldrich, St. Louis, MO). Tissue homogenates were centrifuged at 4°C for 15 min at 12,000 × g and the supernatant was transferred into a new tube. Extracts were stored at −80°C. Equal amounts of protein (50 μg)

were mixed with loading buffer (0.125 M Tris-HCl (pH 6.8), 20% glycerol, 4% SDS, 10% 2-ME, and 0.002% bromphenol blue), boiled for 5 min, and separated by SDS-PAGE. After electrophoresis, proteins were transferred to polyvinylidene difluoride membranes (EMD Millipore) using an electrophoretic transfer system (Bio-Rad Laboratories, Hercules, CA). Membranes were then washed with TBS and blocked for 1 h with TBS containing 5% skim milk. Membranes were then incubated overnight at 4°C with one of the following primary antibodies: rabbit anti-SOCS3 (1:2,000; abcam), rabbit anti-phospho-STAT3 Tyr705 (Cell Signaling Technology), rabbit anti-Bax (1:1,000; Cell Signaling), or rabbit anti-cleaved caspase-3 (Cell Signaling Technology). After washing, membranes were incubated for 1 h at room temperature with HRP-conjugated secondary antibodies (1:10,000; Amersham Biosciences, Pittsburgh, PA) and washed again with TBS. Finally, immunoreactivity was developed using Pierce ECL® or SuperSignal® West Dura substrate (Thermo Scientific). Blots were then re-probed with antibody against β-actin (1:4,000; Cell Signaling Technology), STAT3 (1:1,000; Cell Signaling Technology), or caspase-3 (1:1,000; Cell Signaling Technology). The densities of bands on immunoblots were measured using ImageJ software for further quantitative analyses.

RNA isolation and quantitative real time-PCR

Spinal cord tissues were obtained from areas 5 mm rostral and caudal to the epicenter at the indicated time points after injury and total RNA was extracted using Trizol (Life Technologies). Purified RNA (500 ng) was reverse transcribed into cDNA using Multiscribe reverse transcriptase and random primers (Applied Biosystems by Life Technologies). Quantitative real-time PCR (qRT-PCR) to determine levels of SOCS3 mRNA was performed as previously described (Park et al., 2012). Data were analyzed using the comparative cycle threshold method to obtain quantitative values.

Quantitative analysis of spinal cord neurons

The number of neurons surrounding the injured spinal cord was assessed by examining sections obtained from areas 4 mm rostral and caudal to the injury site. One of every six serial sections (180 μm apart) was selected to avoid double cell counting and was immunostained with NeuN antibody to count NeuN-positive neurons (NeuN+ neurons) in the spinal cord. NeuN+ neurons of spinal cord were counted using a fluorescence microscope at a magnification of 200× and expressed as the number of total spinal cord neurons in each section. Only neurons with normal visible nuclei stained by DAPI were counted.

Measurement of the size of NeuN + neurons

As described above, one of every six serial sections (180 μm apart) were selected, immunostained with NeuN antibody, and digital photomicrographs of NeuN+ neurons in the ventral horn area were then taken with a Leica microscope (DM6000). For measurement of neuronal size, pictures were analyzed by LAS AF software (Leica Microsystems) and the diameter of the individual NeuN+ neurons were measured (Kishino et al., 1997). A total of ~200–230 neurons (10–12 neurons in each section) in each area rostral and caudal to the injury site were measured and analyzed.

Statistical analysis

All values are presented as mean ± SEM. Statistical significance ($p<0.05$ for all analyses) between groups was assessed by ANOVA using GraphPad Prism 5.01 (GraphPad, San Diego, CA), followed by Student–Newman–Keuls analyses. All experimental procedures and data analyses were performed in a blinded fashion over the entire study.

RESULTS

T8 complete SCI induces SOCS3 expression

Levels of SOCS3 mRNA and protein from areas 5 mm rostral and caudal to the T8 injury site were determined at 1, 2, 4, 7 and 14 days after complete SCI. Quantitative-PCR results showed that basal expression levels of SOCS3 mRNA were very low in the T8 spinal cord of sham animals. However, overall SOCS3 mRNA significantly increased during the two week period following complete SCI (Fig. 1A; $p<0.001$). SOCS3 mRNA expression at 1 day post-SCI immediately increased 90- and 130-fold compared to controls in rostral and caudal areas, respectively. After reaching peak levels 1 day post-SCI, SOCS3 expression started to gradually decrease until 14 days post-SCI in areas both rostral and caudal to the injury site (Fig. 1A). For SOCS3 protein expression, immunoblot analysis also demonstrated significant up-regulation of SOCS3 expression at 1, 2, and 4 days post-SCI (Fig. 1B; $p < 0.001$). At 2 days post-SCI, SOCS3 protein reached peak levels, 10.7–10.8-fold higher than sham animals, and then slowly decreased until 14 days post-SCI in areas both rostral and caudal to the injury site.

The majority of SOCS3 was expressed by neurons after T8 complete SCI

We further determined which cell types contributed to SOCS3 over-expression after SCI. The time point of 2 days post-SCI was selected for this purpose because SOCS3 protein expression peaked at this time point (Fig. 1). To identify cells that expressed SOCS3 in areas rostral and caudal to the T8 SCI site, double-immunofluorescence staining of SOCS3 with either NeuN for neurons (Fig. 2A), OX-42 for microglia (Fig. 2B), or glial fibrillary acidic protein (GFAP) for astrocytes (Fig. 2C) was performed. Increased immunofluorescence of SOCS3 was detected 2 days post-SCI (Fig. 2), consistent with the data obtained from immunoblot analysis (Fig. 1B). The results of double-immunofluorescence staining of the same tissue sections revealed that SCI-induced SOCS3 expression was localized primarily in NeuN+ neurons (Fig. 2A), with SOCS3 expressed by OX-42+ microglia (Fig. 2B) to a much lesser extent and no observed SOCS3 expression by GFAP+ astrocytes (Fig. 2C). Extensive analysis of the expression levels and distribution of SOCS3 showed that SCI-induced SOCS3 was mainly expressed by NeuN+ neurons in areas both rostral and caudal to the injury epicenter (Fig. 2D).

STAT3 activation after T8 complete SCI

Previous studies have demonstrated that SOCS3 expression can be induced by the JAK/STAT signaling pathway, particularly STAT3 (Baker et al., 2009; Ma et al., 2010), indicating that SOCS3 is a STAT3-inducible gene. Specifically, phosphorylated STAT3 needs to be dimerized and translocate to the nucleus, where it induces transcription of

SOCS3 genes. Thus, we investigated whether T8 spinal cord complete transection induces tyrosine phosphorylation of STAT3 (P-STAT3 Tyr) *in vivo* as evidence of an essential signaling pathway for SOCS3 expression. Immunoblotting demonstrated that total STAT3 expression was not changed after T8 complete SCI (Fig. 3A). However, increased expression of P-STAT3 Tyr by SCI was significantly induced as early as 1 day, which was maintained up to 2 weeks in areas both rostral and caudal to the injury site (Fig. 3A). The P-STAT3 Tyr reached peak levels 1 day post-SCI, which was 30 and 34 times higher than that of sham animals in rostral and caudal areas, respectively. To test the cellular localization of phosphorylated STAT3, transverse sections of spinal cord from both rostral and caudal segments were examined by double immunofluorescence staining of NeuN with P-STAT3 Tyr. The results showed that P-STAT3 Tyr was detected in NeuN+ neurons and accumulated in nuclei 2 days post-SCI (Fig. 3B). Thus SCI-induced increases in the expression of both P-STAT3 Tyr and SOCS3, which reached peak levels 1 day (Fig. 3A) and 2 days (Fig. 1B) post-SCI, respectively, support the previous findings that SOCS3 is an activity-dependent and STAT3-inducible gene in neurons.

Increased SOCS3 expression contributes to spinal cord neuronal death after T8 complete SCI

SOCS3 expression in neurons was shown to contribute to excitotoxic neuronal death *in vitro* (Park et al., 2012). In order to determine the correlation of up-regulation of SOCS3 with neuronal death after SCI *in vivo*, we investigated the expression of several cell death markers, including Bax and caspase-3. Several studies have demonstrated that increased Bax in spinal cord contributes to contusive SCI-induced Bax-dependent caspase-3 activation (Cregan et al., 1999) and neuronal cell death *in vivo* and *in vitro* (Kotipatruni et al., 2011). Therefore, we first examined the protein expression of Bcl-2 and Bax at 1, 2, 4, 7, and 14 days after complete SCI by western blot analysis in both rostral and caudal spinal cords. Indeed, Bax expression was significantly induced by SCI, while no significant difference was seen in anti-apoptotic Bcl-2 expression, leading to an increased ratio of Bax/Bcl-2. Such changes were similarly found in areas both rostral and caudal to the injured site at all time points examined after SCI (Fig. 4A).

In addition to Bax and Bcl-2, caspase-3 has been shown to be an important marker of apoptotic cell death in spinal cord neurons (Wu et al., 2007). Immunoblot analysis showed that cleaved caspase-3 (the 17kDa active form of caspase-3) expression started to significantly increase at 1 day and continued to 14 days in rostral and caudal cord after complete SCI. Specifically, the induction of cleaved caspase-3 peaked at 7 days and the SCI-induced increases in cleaved caspase-3 were seen in areas both rostral and caudal to the injured site at each individual time point examined after SCI (Fig. 4B). To determine if SCI-induced up-regulation of cleaved caspase-3 occurred in neurons, double-immunofluorescence staining of cleaved caspase-3 with NeuN was performed 7 days after SCI. The results revealed that increased cleaved caspase-3 immunofluorescence was observed mainly in NeuN+ neurons in spinal cord (Fig. 4C), indicating that caspase-3 was involved in SCI-induced neuronal death.

To further evaluate SCI-induced neuronal death, spinal cord tissues harvested 7 days post-SCI were processed for staining with TUNEL and NeuN to visualize nuclear DNA cleavage during cell death of spinal cord neurons. Seven days post-SCI was selected because SCI-induced increases in both Bax/Bcl-2 (Fig. 4A) and cleaved caspase-3 (Fig. 4B) peaked at this time. As shown, there were no TUNEL-positive cells in sham animals (con). TUNEL-positive cells were observed in both gray and white matter after complete SCI. Double staining of NeuN with TUNEL further confirmed neuronal cell death in the gray matter after SCI (Fig. 4D). Together, the peak expression of SOCS3 and P-STAT3 Tyr were observed 1–4 days after SCI and were followed by peak expression of cell death markers (Bax/Bcl-2 and cleaved caspase-3) at 7 days after SCI (Fig. 4E). These data indicated that early expression of SOCS3 and P-STAT3 Tyr by neurons contributed to subsequent neuronal death after T8 complete SCI.

Reduction of SCI-induced SOCS3 expression contributed to neuroprotective effects after complete SCI

To investigate if manipulation of SOCS3 levels prevents further neuronal death after complete SCI, we applied shSOCS3 2 weeks prior to complete SCI to inhibit SOCS3 expression after SCI. As the infection efficiency of lentivirus in neurons has been debated (Karra and Dahm, 2010; Peluffo et al., 2013), we first tested whether spinal cord neurons were infected by our lentivirus preparation *in vivo*. Control lentivirus tagged with Green Fluorescence Protein (GFP) was injected into T8 spinal cord gray matter. Two weeks later animals were sacrificed and analyzed by immunofluorescence staining with NeuN. The results revealed that GFP immunoreactivity was co-localized within NeuN+ neurons (Fig. 5A), indicating the major infected cell type by lentivirus is neurons. The animals that received shSOCS3 showed a significant reduction (~30%) of SOCS3 mRNA expression 2 days after complete SCI, the time point showing highest SOCS3 expression (Fig. 1B), compared to animals with control lentvirus (pGipz) treatment, which was found similarly in both rostral and caudal spinal cord segments (Fig. 5B). In addition, shSOCS3 microinjection significantly decreased the Bax/Bcl-2 ratio in the spinal cord both rostral (~30%) and caudal (~50%) to the lesion epicenter 7 days post-SCI, the time point with the greatest SCI-induced Bax/Bcl-2 ratio (Fig. 4A), when compared to animals with control lentivirus treatment (Figs. 5C and 5D). Moreover, we analyzed the number of NeuN+ neurons in the gray matter 7 days post-SCI, the time point with the peak value of neuronal death, to further test the neuroprotective efficacy of shSOCS3 intervention. As shown, significant more NeuN+ neurons were seen in the spinal cord gray matter of shSOCS3-treated animals as compared to control lentivirus (pGipz)-treated animals (Fig. 6A). Quantitative analysis demonstrated that shSOCS3 treatment reduced SCI-induced neuronal death in both rostral and caudal spinal cord as compared to control lentivirus treatment (Fig. 6B). Furthermore, analysis of cell size of NeuN+ neurons in the ventral horn of T8 spinal cord demonstrated that shSOCS3 treatment rescued SCI-induced neuronal cell damage in both rostral and caudal spinal cord, as compared to control lentivirus treatment (Fig. 6C). These data suggested that a reduction of endogenous SOCS3 in neurons can prevent further neuronal death after complete SCI.

DISCUSSION

The present study investigates the pattern of SOCS3 expression in neurons and its negatively regulatory effects on antiapoptotic protein expression, which consequently contributes to neuronal death after complete SCI in adult rats. Complete SCI at T8 induces SOCS3 expression in spinal cord neurons both rostral and caudal to the injured site, which is also accompanied by STAT3 activation for transcription of SOCS3. Results from experiments using shSOCS3 to inhibit endogenous SOCS3 expression demonstrate that SOCS3 functions as a regulator of SCI-induced cell death-related protein expression, which subsequently leads to deleterious effects on SCI-induced neuronal death. The current results are the first to demonstrate that (1) endogenous SOCS3 expression in spinal cord neurons contributes to SCI-induced neuronal death, (2) inhibition of endogenous SOCS3 expression reduces pro-apoptotic Bax proteins and Bax/Bcl-2 levels after SCI in spinal cord neurons, and (3) inhibition of endogenous SOCS3 expression in spinal cord neurons prevents further neuronal death after T8 complete SCI in adult rats.

SOCS3 as a potential target to prevent neuronal death after SCI

SCI leads to a series of cellular and molecular events that results in primary tissue destruction and a subsequent secondary injury cascade (Beattie et al., 2002; Beattie, 2004), including excitotoxicity, oxidative stress, axonal degeneration, demyelination and enhanced cell death of neurons and glia (Lu et al., 2000; Hausmann, 2003). Secondary injury can start after primary tissue damage and gradually spread over time both rostral and caudal to the primary injury site (Liu et al., 1997; Oyinbo, 2011). Previous studies have revealed an extensive therapeutic window during the intermediate phase of secondary injury progression (Oyinbo, 2011). The outcome of traumatic SCI depends significantly on the ability of exogenous intervention within this therapeutic window to prevent the progression of secondary injury. In the present study, we have demonstrated the immediate induction of SOCS3 mRNA expression at one day post-complete SCI, reaching peak protein levels at 2 days; this was followed by ~50% of neuronal death after 7 days of SCI. Therefore, inhibiting SOCS3 expression at an acute stage to prevent further neuronal death is a critical step. In addition, we have identified significant neuronal death within areas 4 mm rostral and caudal to the injured site. We have previously demonstrated functional recovery and regenerative nerve fibers within 5 mm areas beyond the lesion site with our peripheral nerve bridging strategy after complete SCI (Lee et al., 2002; Lee et al., 2004; Lee et al., 2006; Lee et al., 2013). Therefore, promoting neuronal survival within a 4 mm range could be critical for improving functional outcomes when combined with a nerve regenerative strategy.

Involvement of Bax/Bcl-2 and caspase-3 in neuronal death after SCI

Neuronal apoptotic cell death after SCI is one of the most severe results, which can cause neuronal loss and functional deficits (Profyris et al., 2004; Teng et al., 2004). The Bcl-2 family of proteins, which includes pro-apoptotic Bax and anti-apoptotic Bcl-2, plays an important role in mediating apoptotic cell death (Ola et al., 2011; Rahman et al., 2012). Bax forms heterodimers with Bcl-2 and the ratio of Bax/Bcl-2 determines if cell death occurs after apoptotic stimuli (Oltvai et al., 1993; Ola et al., 2011). In our experiments, significant increases in Bax expression resulting in increases in the Bax/Bcl-2 ratio were observed after

SCI. Thus, we hypothesized that the appropriate balance between Bax and Bcl-2 is disturbed in spinal cord after injury, leading to neuronal cell death due to increased Bax expression. Furthermore, activation of caspase-3 confirmed neuronal apoptotic cell death after SCI, as caspase-3 is implicated in the execution of apoptotic cell death in neurons (Yuan and Yankner, 2000; Ola et al., 2011). Significantly, recent studies reported neuronal cell death, characterized by chromatin condensation and DNA fragmentation (Stirling et al., 2004; Wu et al., 2007), was also observed after complete SCI using TUNEL assays. These *in vivo* data strongly support the hypothesis that Bax expression and activation of caspase-3 are key mediators of apoptotic neuronal death after SCI.

Bcl-2 expression as STAT3 transcription target gene

Phosphorylated STAT3 dimerizes and translocates to the nucleus, where it induces transcription of target genes including Bcl-xL, Bcl-2 and survivin, which are critical for promoting neuronal survival (Dziennis and Alkayed, 2008; Guo et al., 2008). The structure of STAT3 is comprised of an amino terminal, a DNA binding domain, SH2 and a transcriptional activation domain. The DNA binding domain recognizes the consensus binding regions on gene promoters. STAT3 binding sites are present in the anti-apoptotic genes Bcl-2 and Bcl-xL (Stephanou et al., 2000). A recent study reported that in STAT3 conditional knockout mice, neuron-specific gene ablation of STAT3 reduced Bcl-2 expression after nerve injury (Schweizer et al., 2002), indicating that Bcl-2 is a STAT3-inducible gene. Collectively, these results indicate that activation of STAT3 can induce Bcl-2 expression as a transcription target gene, which consequently promotes neuronal survival.

Regulation of the STAT3/SOCS3 pathway and neuronal death after SCI

SCI triggers secondary injury cascades, including expression of inflammatory mediators such as IL-1, TNF-α, and IL-6. A number of studies have reported that the IL-6 cytokine family can induce phosphorylation of STAT3 in neurons (Sango et al., 2008; Park et al., 2012; Leibinger et al., 2013). A recent study demonstrated that SCI-induced IL-6 is mainly expressed in neurons, which activates the Jak/ STAT pathway (Yamauchi et al., 2006). Taken together, these results suggest that SCI induces upregulation of IL-6 expression, which can mediate phosphorylation of STAT3 in neurons. Furthermore, this hypothesis is supported by a recent study showing that neutralizing of IL-6 reduces nerve injury-induced phosphorylation of STAT3 in the spinal cord (Dominguez et al., 2010). However, there are a number of studies showing that NGF, cAMP, IGF-1, leptin, and nerve injury can also induce neuronal STAT3 activation *in vivo* and *in vitro* (Guo et al., 2008; Miao et al., 2006; Yadav et al., 2005; Zhou and Too, 2011). These results suggest that several inflammatory mediators, secreted or elevated after SCI, can activate STAT3 signaling in spinal cord neurons.

One of the major functions of SOCS3 is to limit signaling by inhibiting JAK tyrosine kinase activity, thereby preventing STAT3 activation (Croker et al., 2003; Lang et al., 2003). As SOCS3 deficiency is embryonic lethal (Roberts et al., 2001) and currently pharmacological inhibitors are not available, conditional gene targeting was used to inhibit the function of SOCS3 in our studies. Targeted deletion of SOCS3 in mouse brain and cultured neurons leads to elevated STAT3 activation (Miao et al., 2006; Miao et al., 2008; Ernst et al., 2009).

In addition, SOCS3 in neurons has been reported to inhibit cytokine-induced STAT3 activation and the inducible gene, Bcl-xL, while inhibition of SOCS3 enhances STAT3 activation (Park et al., 2012). SOCS3 expression, however, is known to be inducible by STAT3, as STAT3 activation is necessary for SOCS3 expression *in vitro* (Park et al., 2012). These data suggest that phosphorylation of STAT3 after spinal cord transection can induce SOCS3 expression *in vivo*.

Activated STAT3 functions as a key effector of neuronal survival after injury to neural tissue, in part by inducing anti-apoptotic genes such as Bcl-2, Bcl-xL and Mn-SOD (Dziennis and Alkayed, 2008; Sun and He, 2010; Park et al., 2012). However, STAT3 activation also leads to induction of SOCS3, which functions as a negative feedback modulator to the JAK/STAT3 pathway. The functional consequences of SOCS3 expression include inhibition of STAT3 activation and inhibition of anti-apoptotic molecules, including Bcl-2 and Bcl-xL. All of these contribute to loss of the protective effects of STAT3 on neuronal survival (Fig. 7A). In the present study, we did not observe clear up-regulation of Bcl-2 expression, whereas Bax expression was significantly inhibited after SOCS3 was inhibited by shSOCS3. However, a previous study reported that Bax binds to Bcl-2 and that the Bax/Bcl-2 ratio determines cell death following apoptotic stimuli (Oltvai et al., 1993). Therefore, reduction of the Bax/Bcl-2 ratio by inhibition of SOCS3 expression in the current study can be a targeting mechanism for preventing further neuronal death after SCI (Fig. 7B). Further studies will be required to investigate the possible mechanism of interaction between SOCS3 and Bax expression.

Different roles for SOCS3 depending on the cell type involved

SOCS3 was reported to play different roles in the central nervous system depending on the cell type examined (Baker et al., 2009). Several lines of evidence suggest that in microglia, SOCS3 inhibits cytokine-induced immune and inflammatory responses *in vitro* (Qin et al., 2006; Qin et al., 2007) and in astrocytes SOCS3 enhances inhibition of chemokine expression and T-cell migration (Ma et al., 2010). Additionally, in an animal model of multiple sclerosis, SOCS3 expression in microglia and macrophages is critical for deactivation of neuroinflammatory responses and protection of neurons (Qin et al., 2012). Furthermore, lentiviral-induced SOCS3 expression in spinal cord microglia attenuates neuroinflammation and blocks the development of mechanical allodynia (Dominguez et al., 2010). Thus, these data collectively suggest that SOCS3 expression in microglia, macrophages and astrocytes suppress brain inflammation. It remains to be determined what the role of SOCS3 is in activated microglia after SCI. The role of SOCS3 in neurons is detrimental for STAT3-induced neuroprotection, as OSM or IL-6 + IL-6R-induced SOCS3 expression in neurons was reported to inhibit STAT3-induced protective effects on neurons *in vitro* (Park et al., 2012). These results are supported by our findings that SCI-induced SOCS3 is mainly expressed by neurons and that increased SOCS3 expression is involved in SCI-induced neuronal death *in vivo*. Given that the function of SOCS3 is cell-type specific, it is thus important to understand how to selectively inhibit SOCS3 expression in neurons and to induce SOCS3 in microglia as a therapeutic target following SCI.

Conclusion

In conclusion, the results from this investigation of SOCS3 expression with cell death markers demonstrate the contribution of SOCS3 to neuronal death after complete SCI. Conditionally knocking down endogenous SOCS3 levels provides neuroprotective effects after SCI. These data suggest that SOCS3 can be used as a potential target to develop a strategy to treat SCI. Further studies will be needed to investigate the efficacy of neuroprotection or functional improvement to deliver shSOCS3 after SCI.

Acknowledgments

This project was funded by a grant from the National Institute of Neurological Disorders and Stroke NS069765 (to Y-S. Lee)

REFERENCES

Baker BJ, Akhtar LN, Benveniste EN. SOCS1 and SOCS3 in the control of CNS immunity. Trends Immunol. 2009; 30:392–400. [PubMed: 19643666]

Beattie MS, Hermann GE, Rogers RC, Bresnahan JC. Cell death in models of spinal cord injury. Prog Brain Res. 2002; 137:37–47. [PubMed: 12440358]

Beattie MS. Inflammation and apoptosis: linked therapeutic targets in spinal cord injury. Trends Mol Med. 2004; 10:580–583. [PubMed: 15567326]

Cregan SP, MacLaurin JG, Craig CG, Robertson GS, Nicholson DW, Park DS, Slack RS. Bax-dependent caspase-3 activation is a key determinant in p53-induced apoptosis in neurons. J Neurosci. 1999; 19:7860–7869. [PubMed: 10479688]

Croker BA, Krebs DL, Zhang JG, Wormald S, Willson TA, Stanley EG, Robb L, Greenhalgh CJ, Forster I, Clausen BE, Nicola NA, Metcalf D, Hilton DJ, Roberts AW, Alexander WS. SOCS3 negatively regulates IL-6 signaling in vivo. Nat Immunol. 2003; 4:540–545. [PubMed: 12754505]

Dominguez E, Mauborgne A, Mallet J, Desclaux M, Pohl M. SOCS3-mediated blockade of JAK/STAT3 signaling pathway reveals its major contribution to spinal cord neuroinflammation and mechanical allodynia after peripheral nerve injury. J Neurosci. 2010; 30:5754–5766. [PubMed: 20410127]

Dziennis S, Alkayed NJ. Role of signal transducer and activator of transcription 3 in neuronal survival and regeneration. Rev Neurosci. 2008; 19:341–361. [PubMed: 19145989]

Ernst MB, Wunderlich CM, Hess S, Paehler M, Mesaros A, Koralov SB, Kleinridders A, Husch A, Munzberg H, Hampel B, Alber J, Kloppenburg P, Bruning JC, Wunderlich FT. Enhanced Stat3 activation in POMC neurons provokes negative feedback inhibition of leptin and insulin signaling in obesity. J Neurosci. 2009; 29:11582–11593. [PubMed: 19759305]

Guo Z, Jiang H, Xu X, Duan W, Mattson MP. Leptin-mediated cell survival signaling in hippocampal neurons mediated by JAK STAT3 and mitochondrial stabilization. J Biol Chem. 2008; 283:1754–1763. [PubMed: 17993459]

Hausmann ON. Post-traumatic inflammation following spinal cord injury. Spinal Cord. 2003; 41:369–378. [PubMed: 12815368]

Karra D, Dahm R. Transfection techniques for neuronal cells. J Neurosci. 2010; 30:6171–6177. [PubMed: 20445041]

Kishino A, Ishige Y, Tatsuno T, Nakayama C, Noguchi H. BDNF prevents and reverses adult rat motor neuron degeneration and induces axonal outgrowth. Exp Neurol. 1997; 144:273–286. [PubMed: 9168829]

Kotipatruni RR, Dasari VR, Veeravalli KK, Dinh DH, Fassett D, Rao JS. p53- and Bax-mediated apoptosis in injured rat spinal cord. Neurochem Res. 2011; 36:2063–2074. [PubMed: 21748659]

Lang R, Pauleau AL, Parganas E, Takahashi Y, Mages J, Ihle JN, Rutschman R, Murray PJ. SOCS3 regulates the plasticity of gp130 signaling. Nat Immunol. 2003; 4:546–550. [PubMed: 12754506]

Lee YS, Hsiao I, Lin VW. Peripheral nerve grafts and aFGF restore partial hindlimb function in adult paraplegic rats. Journal of neurotrauma. 2002; 19:1203–1216. [PubMed: 12427329]

Lee YS, Lin CY, Robertson RT, Hsiao I, Lin VW. Motor recovery and anatomical evidence of axonal regrowth in spinal cord-repaired adult rats. J Neuropathol Exp Neurol. 2004; 63:233–245. [PubMed: 15055447]

Lee YS, Lin CY, Robertson RT, Yu J, Deng X, Hsiao I, Lin VW. Re-growth of catecholaminergic fibers and protection of cholinergic spinal cord neurons in spinal repaired rats. Eur J Neurosci. 2006; 23:693–702. [PubMed: 16487151]

Lee YS, Lin CY, Jiang HH, Depaul M, Lin VW, Silver J. Nerve regeneration restores supraspinal control of bladder function after complete spinal cord injury. J Neurosci. 2013; 33:10591–10606. [PubMed: 23804083]

Leibinger M, Muller A, Gobrecht P, Diekmann H, Andreadaki A, Fischer D. Interleukin-6 contributes to CNS axon regeneration upon inflammatory stimulation. Cell death & disease. 2013; 4:e609. [PubMed: 23618907]

Liu XZ, Xu XM, Hu R, Du C, Zhang SX, McDonald JW, Dong HX, Wu YJ, Fan GS, Jacquin MF, Hsu CY, Choi DW. Neuronal and glial apoptosis after traumatic spinal cord injury. J Neurosci. 1997; 17:5395–5406. [PubMed: 9204923]

Lu J, Ashwell KW, Waite P. Advances in secondary spinal cord injury: role of apoptosis. Spine (Phila Pa 1976). 2000; 25:1859–1866. [PubMed: 10888960]

Ma X, Reynolds SL, Baker BJ, Li X, Benveniste EN, Qin H. IL-17 enhancement of the IL-6 signaling cascade in astrocytes. J Immunol. 2010; 184:4898–4906. [PubMed: 20351184]

Miao T, Wu D, Zhang Y, Bo X, Subang MC, Wang P, Richardson PM. Suppressor of cytokine signaling-3 suppresses the ability of activated signal transducer and activator of transcription-3 to stimulate neurite growth in rat primary sensory neurons. J Neurosci. 2006; 26:9512–9519. [PubMed: 16971535]

Miao T, Wu D, Zhang Y, Bo X, Xiao F, Zhang X, Magoulas C, Subang MC, Wang P, Richardson PM. SOCS3 suppresses AP-1 transcriptional activity in neuroblastoma cells through inhibition of c-Jun N-terminal kinase. Mol Cell Neurosci. 2008; 37:367–375. [PubMed: 18055217]

Nicholson SE, De Souza D, Fabri LJ, Corbin J, Willson TA, Zhang JG, Silva A, Asimakis M, Farley A, Nash AD, Metcalf D, Hilton DJ, Nicola NA, Baca M. Suppressor of cytokine signaling-3 preferentially binds to the SHP-2-binding site on the shared cytokine receptor subunit gp130. Proc Natl Acad Sci U S A. 2000; 97:6493–6498. [PubMed: 10829066]

Ola MS, Nawaz M, Ahsan H. Role of Bcl-2 family proteins and caspases in the regulation of apoptosis. Mol Cell Biochem. 2011; 351:41–58. [PubMed: 21210296]

Oltvai ZN, Milliman CL, Korsmeyer SJ. Bcl-2 heterodimerizes in vivo with a conserved homolog, Bax, that accelerates programmed cell death. Cell. 1993; 74:609–619. [PubMed: 8358790]

Oyinbo CA. Secondary injury mechanisms in traumatic spinal cord injury: a nugget of this multiply cascade. Acta Neurobiol Exp (Wars). 2011; 71:281–299. [PubMed: 21731081]

Park KW, Nozell SE, Benveniste EN. Protective role of STAT3 in NMDA and glutamate-induced neuronal death: negative regulatory effect of SOCS3. PloS one. 2012; 7:e50874. [PubMed: 23226414]

Peluffo H, Foster E, Ahmed SG, Lago N, Hutson TH, Moon L, Yip P, Wanisch K, Caraballo-Miralles V, Olmos G, Lladó J, McMahon SB, Yáñez-Muñoz RJ. Efficient gene expression from integration-deficient lentiviral vectors in the spinal cord. Gene Ther. 2013; 20:645–657. [PubMed: 23076378]

Profyris C, Cheema SS, Zang D, Azari MF, Boyle K, Petratos S. Degenerative and regenerative mechanisms governing spinal cord injury. Neurobiol Dis. 2004; 15:415–436. [PubMed: 15056450]

Qin H, Wilson CA, Roberts KL, Baker BJ, Zhao X, Benveniste EN. IL-10 inhibits lipopolysaccharide-induced CD40 gene expression through induction of suppressor of cytokine signaling-3. J Immunol. 2006; 177:7761–7771. [PubMed: 17114447]

Qin H, Roberts KL, Niyongere SA, Cong Y, Elson CO, Benveniste EN. Molecular mechanism of lipopolysaccharide-induced SOCS-3 gene expression in macrophages and microglia. J Immunol. 2007; 179:5966–5976. [PubMed: 17947670]

Qin H, Yeh WI, De Sarno P, Holdbrooks AT, Liu Y, Muldowney MT, Reynolds SL, Yanagisawa LL, Fox TH, Park K, Harrington LE, Raman C, Benveniste EN. Signal transducer and activator of transcription-3/suppressor of cytokine signaling-3 (STAT3/SOCS3) axis in myeloid cells regulates neuroinflammation. Proc Natl Acad Sci U S A. 2012; 109:5004–5009. [PubMed: 22411837]

Rahman MA, Kim NH, Yang H, Huh SO. Angelicin induces apoptosis through intrinsic caspase-dependent pathway in human SH-SY5Y neuroblastoma cells. Mol Cell Biochem. 2012; 369:95–104. [PubMed: 22766766]

Roberts AW, Robb L, Rakar S, Hartley L, Cluse L, Nicola NA, Metcalf D, Hilton DJ, Alexander WS. Placental defects and embryonic lethality in mice lacking suppressor of cytokine signaling 3. Proc Natl Acad Sci U S A. 2001; 98:9324–9329. [PubMed: 11481489]

Sango K, Yanagisawa H, Komuta Y, Si Y, Kawano H. Neuroprotective properties of ciliary neurotrophic factor for cultured adult rat dorsal root ganglion neurons. Histochemistry and cell biology. 2008; 130:669–679. [PubMed: 18679704]

Schmitz J, Weissenbach M, Haan S, Heinrich PC, Schaper F. SOCS3 exerts its inhibitory function on interleukin-6 signal transduction through the SHP2 recruitment site of gp130. J Biol Chem. 2000; 275:12848–12856. [PubMed: 10777583]

Schweizer U, Gunnersen J, Karch C, Wiese S, Holtmann B, Takeda K, Akira S, Sendtner M. Conditional gene ablation of Stat3 reveals differential signaling requirements for survival of motoneurons during development and after nerve injury in the adult. J Cell Biol. 2002; 156:287–297. [PubMed: 11807093]

Stephanou A, Brar BK, Knight RA, Latchman DS. Opposing actions of STAT-1 and STAT-3 on the Bcl-2 and Bcl-x promoters. Cell death and differentiation. 2000; 7:329–330. [PubMed: 10866494]

Stirling DP, Khodarahmi K, Liu J, McPhail LT, McBride CB, Steeves JD, Ramer MS, Tetzlaff W. Minocycline treatment reduces delayed oligodendrocyte death, attenuates axonal dieback, and improves functional outcome after spinal cord injury. J Neurosci. 2004; 24:2182–2190. [PubMed: 14999069]

Sun F, He Z. Neuronal intrinsic barriers for axon regeneration in the adult CNS. Curr Opin Neurobiol. 2010; 20:510–518. [PubMed: 20418094]

Sun F, Park KK, Belin S, Wang D, Lu T, Chen G, Zhang K, Yeung C, Feng G, Yankner BA, He Z. Sustained axon regeneration induced by co-deletion of PTEN and SOCS3. Nature. 2011; 480:372–375. [PubMed: 22056987]

Teng YD, Choi H, Onario RC, Zhu S, Desilets FC, Lan S, Woodard EJ, Snyder EY, Eichler ME, Friedlander RM. Minocycline inhibits contusion-triggered mitochondrial cytochrome c release and mitigates functional deficits after spinal cord injury. Proc Natl Acad Sci U S A. 2004; 101:3071–3076. [PubMed: 14981254]

Tsujimoto Y. Cell death regulation by the Bcl-2 protein family in the mitochondria. J Cell Physiol. 2003; 195:158–167. [PubMed: 12652643]

Wu KL, Hsu C, Chan JY. Impairment of the mitochondrial respiratory enzyme activity triggers sequential activation of apoptosis-inducing factor-dependent and caspase-dependent signaling pathways to induce apoptosis after spinal cord injury. J Neurochem. 2007; 101:1552–1566. [PubMed: 17298387]

Yadav A, Kalita A, Dhillon S, Banerjee K. JAK/STAT3 pathway is involved in survival of neurons in response to insulin-like growth factor and negatively regulated by suppressor of cytokine signaling-3. J Biol Chem. 2005; 280:31830–31840. [PubMed: 15998644]

Yamauchi K, Osuka K, Takayasu M, Usuda N, Nakazawa A, Nakahara N, Yoshida M, Aoshima C, Hara M, Yoshida J. Activation of JAK/STAT signalling in neurons following spinal cord injury in mice. J Neurochem. 2006; 96:1060–1070. [PubMed: 16417589]

Yoshimura A, Naka T, Kubo M. SOCS proteins, cytokine signalling and immune regulation. Nat Rev Immunol. 2007; 7:454–465. [PubMed: 17525754]

Yuan J, Yankner BA. Apoptosis in the nervous system. Nature. 2000; 407:802–809. [PubMed: 11048732]

Zhou L, Too HP. Mitochondrial localized STAT3 is involved in NGF induced neurite outgrowth. PloS one. 2011; 6:e21680. [PubMed: 21738764]

Highlights

- Complete spinal cord injury increases SOCS3 expression in neurons
- Increased SOCS3 expression correlates with neuronal death after spinal cord injury
- Reduction of spinal cord injury induced SOCS3 expression provides neuroprotection

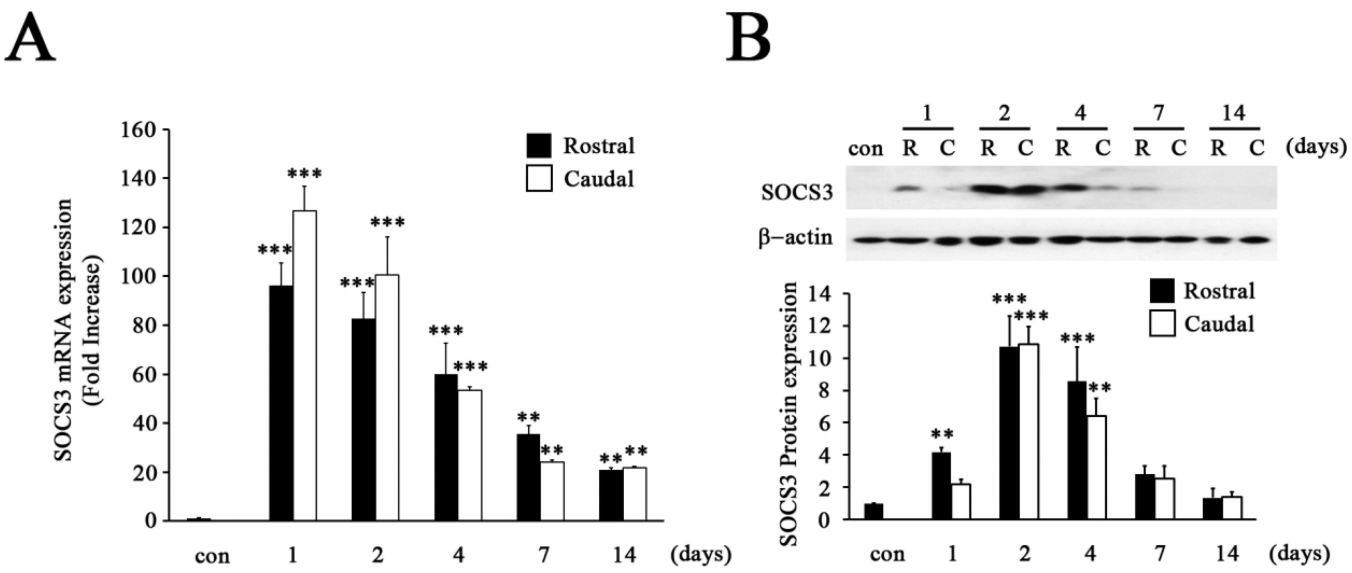

Figure 1. Induction of SOCS3 expression after T8 complete SCI

A, The mRNA expression of SOCS3 was significantly increased after SCI in areas both rostral and caudal to the injured site at 1, 2, 4, 7 or 14 days post-SCI. Graphs represent mean ± SEM of triplicate samples per time point. **p < 0.01, and ***p < 0.001 compared to sham animals (con) (ANOVA and Student-Newman-Keuls analyses). **B**, Expression levels of SOCS3 protein were significantly increased 2 and 4 days after SCI in areas both rostral (R) and caudal (C) to the injured site, then gradually returned to levels similar to controls. Graphs represent mean ± SEM of three to four samples per time point. **p < 0.01, and ***p < 0.001 compared to sham animals (con) (ANOVA and Student-Newman-Keuls analyses).

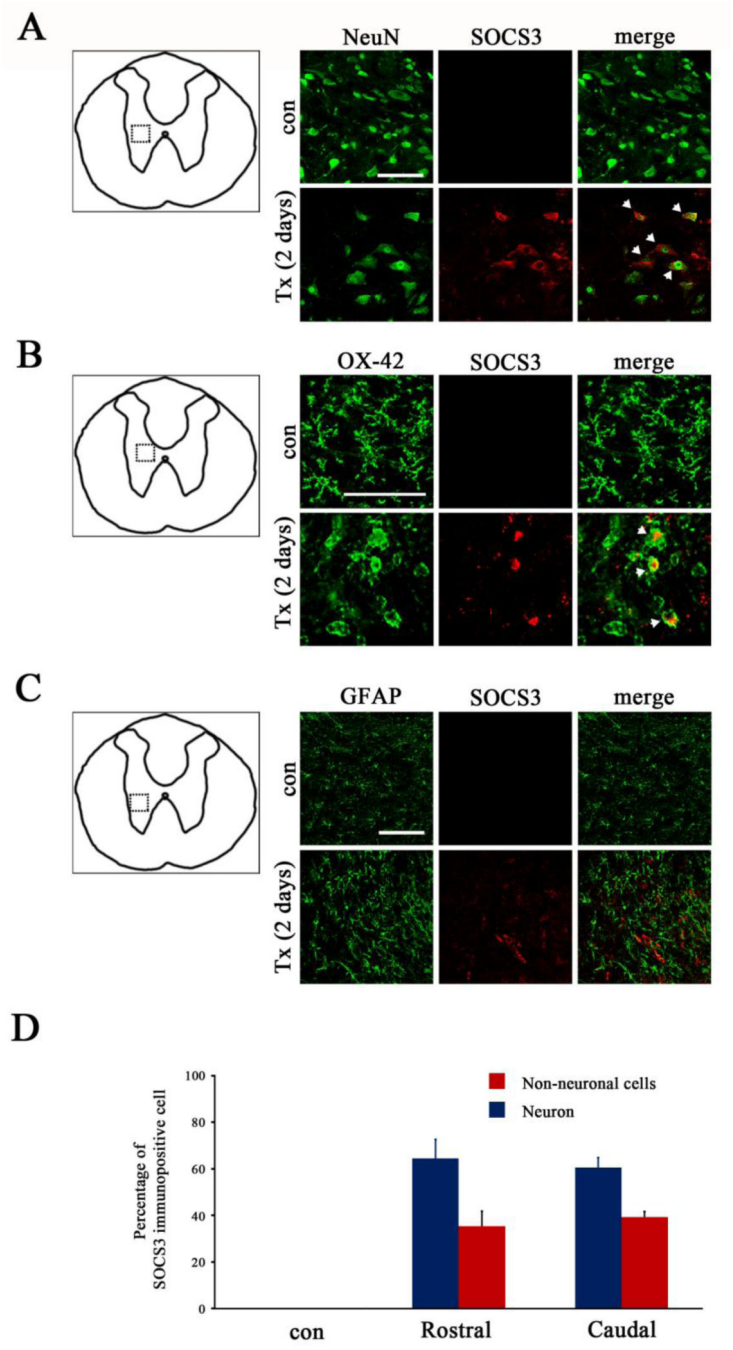

Figure 2. Expression of SOCS3 in neurons and microglia 2 days after T8 complete SCI

A–C, Double staining of SOCS3 (red) with a green fluorescein–conjugated specific marker for neurons (NeuN+, **A**), microglia (OX-42+, **B**) or astrocytes (GFAP+, **C**) showed that SOCS3 was expressed by both NeuN+ neurons (arrow) and OX-42+ activated microglia (arrow) but not by GFAP+ astrocytes 2 days after complete transection (Tx) of T8 spinal cord. The dotted boxes in the schematic diagrams in **A–C** indicate the locations where images were taken. These data are representative of three animals per group. Scale bar, 100

μm. **D**, Neurons were the major cell population expressing SOCS3 in both rostral and caudal spinal cord after SCI. Values represent mean ± SEM (n=3–4 animals in each group).

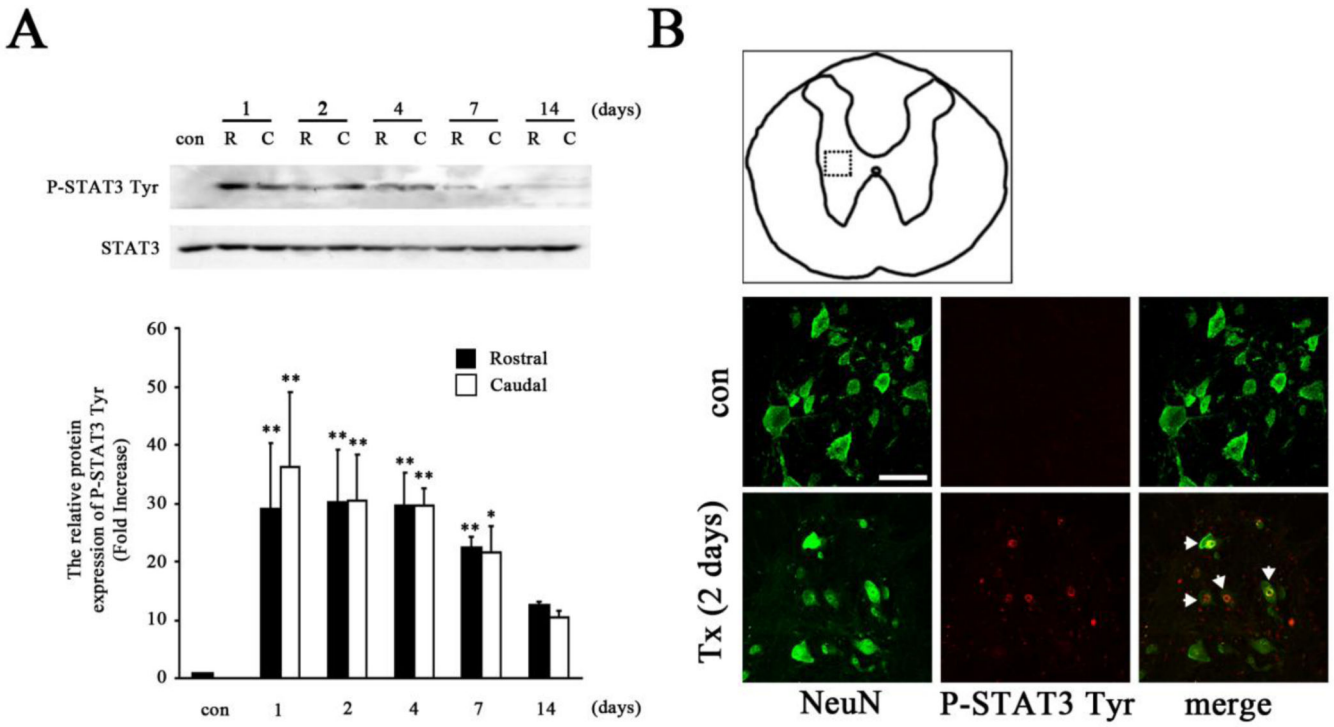

Figure 3. STAT3 activation after T8 complete SCI

A, Western blot analysis showed significant activation of STAT3, indicated by P-STAT3 Tyr expression, in SCI animals. The expression of P-STAT3 Tyr rapidly reached peak values 1 day after SCI in areas both rostral (R) and caudal (C) to the injured site, and then decreased gradually over time to levels that remained higher than those of sham animals (con). Graphs represent mean ± SEM of three to four samples per time point. *$p < 0.05$, **$p < 0.01$, and ***$p < 0.001$ compared to sham animals (ANOVA and Student-Newman-Keuls analyses). **B**, P-STAT3 Tyr immunoreactivity (arrow) was co-localized with NeuN+ neurons 2 days after SCI (Tx). The dotted box in the schematic diagram in **B** indicates the location that images were taken from. Scale bar, 75 μm.

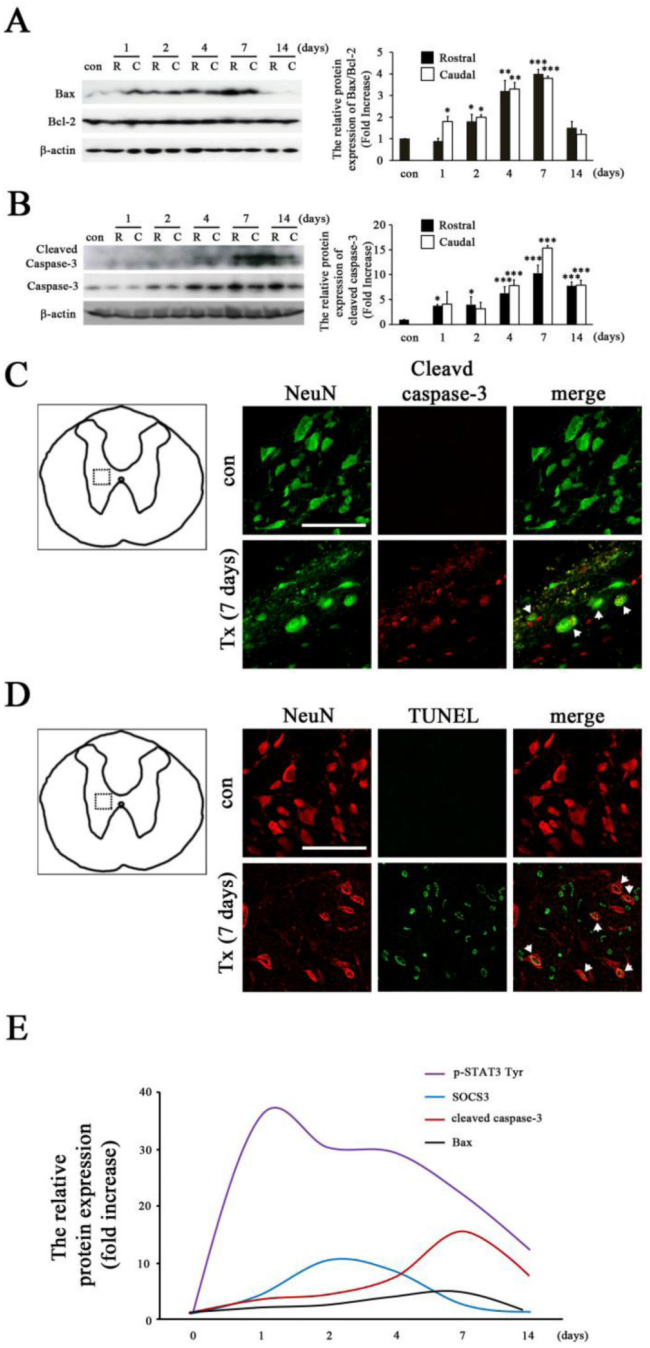

Figure 4. Spinal cord neuronal death after T8 complete SCI

A, Western blot analysis showed significant up-regulation of Bax expression in SCI animals. Graphs represent changes in the ratio of Bax/Bcl-2 in spinal cord after SCI. The ratio of Bax/Bcl-2 was gradually increased after SCI and reached to peak values 7 days after SCI in areas both rostral (R) and caudal (C) to the injured site. Results are presented as mean ± SEM of three samples per time-point. *$p < 0.05$, **$p < 0.01$, and ***$p < 0.001$ compared to sham animals (con) (ANOVA and Student-Newman-Keuls analyses). **B**, Significant up-regulation of cleaved caspase-3 in SCI animals as indicated by western blot analysis. The

peak value of cleaved caspase-3 protein was induced 7 days after SCI in areas both rostral (R) and caudal (C) to the injured site. Graphs represent mean ± SEM of three to four samples per time point. *$p < 0.05$ and ***$p < 0.001$ compared to sham animals (con) (ANOVA and Student-Newman-Keuls analyses). **C**, The expression of SCI-induced cleaved caspase-3 co-localized with NeuN+ neurons (arrow) 7 days after SCI (Tx). **D**, Co-localization of TUNEL+ cells with NeuN+ neurons 7 days after SCI is indicated (arrow). These data are representative of four animals per group. The dotted box in schematic diagrams in **C** and **D** indicate the locations where images were taken. Scale bar, 75 μm. **E**, Relative protein expression of P-STAT3 Tyr, SOCS3, cleaved caspase-3, and Bax after SCI. Note that SCI quickly induced the expression of P-STAT3 Tyr and SOCS3, which was followed by cell death markers such as cleaved caspase-3 and Bax.

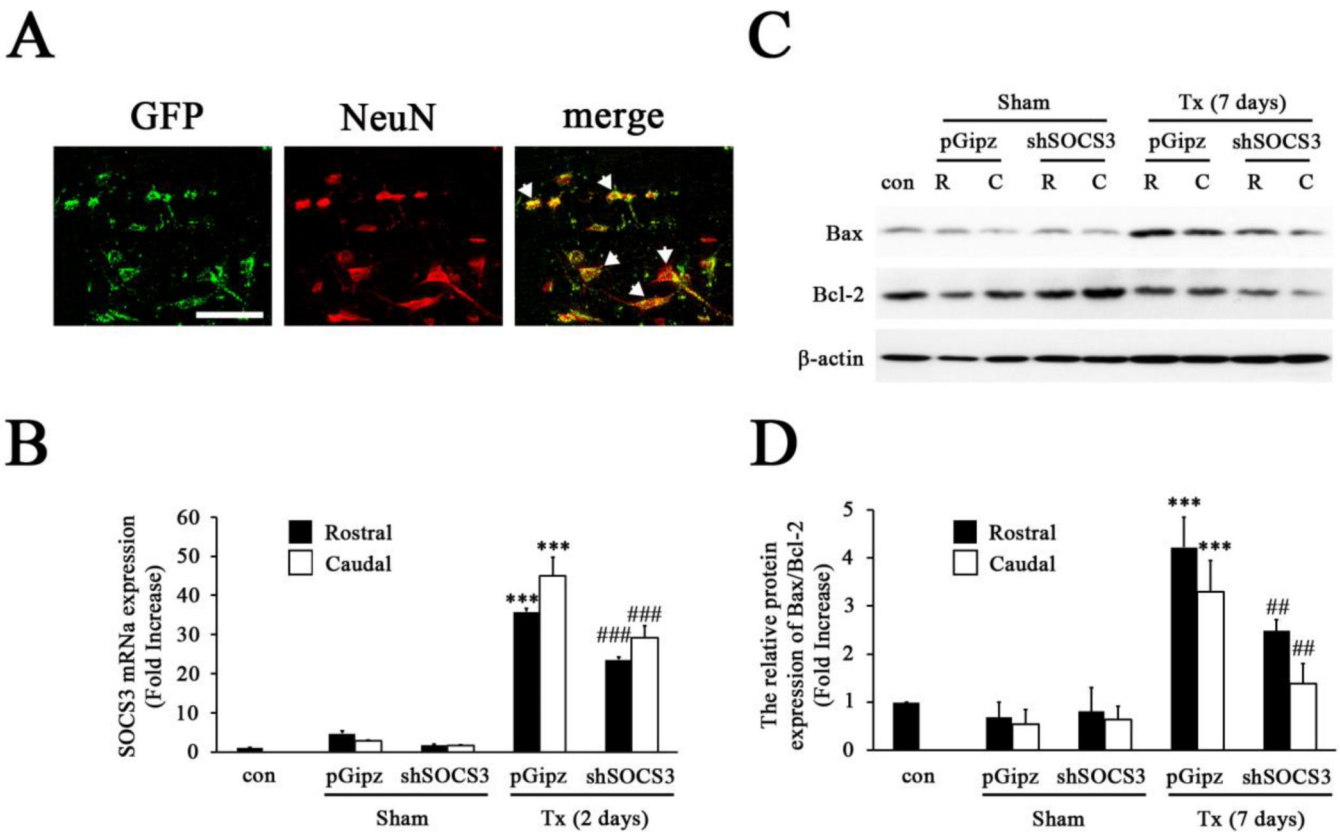

Figure 5. Inhibition of SCI-induced SOCS3 expression by shSOCS3

A, NeuN+ neurons in the spinal cord were found to be infected by GFP-tagged lentivirus (arrow). Scale bar, 25 μm. **B**, Quantitative-PCR analysis of SOCS3 mRNA levels showed that shSOCS3 inhibited SCI-induced increases in endogenous SOCS3 expression 2 days after SCI in areas both rostral and caudal to the injured site. ***$p < 0.001$ compared to sham (con) group; ###$p<0.001$ compared to control lentivirus (pGipz)-treated group (ANOVA and Student-Newman-Keuls analyses). **C–D**, Western blot analysis showed SCI-induced increases in the expression of Bax and that the Bax/Bcl-2 ratio was reduced by shSOCS3 7 days after SCI (Tx) in areas both rostral (R) and caudal (C) to the injured site. ***$p<0.001$ compared to sham (con) group; ##$p<0.01$ compared to pGipz group (ANOVA and Student-Newman-Keuls analyses).

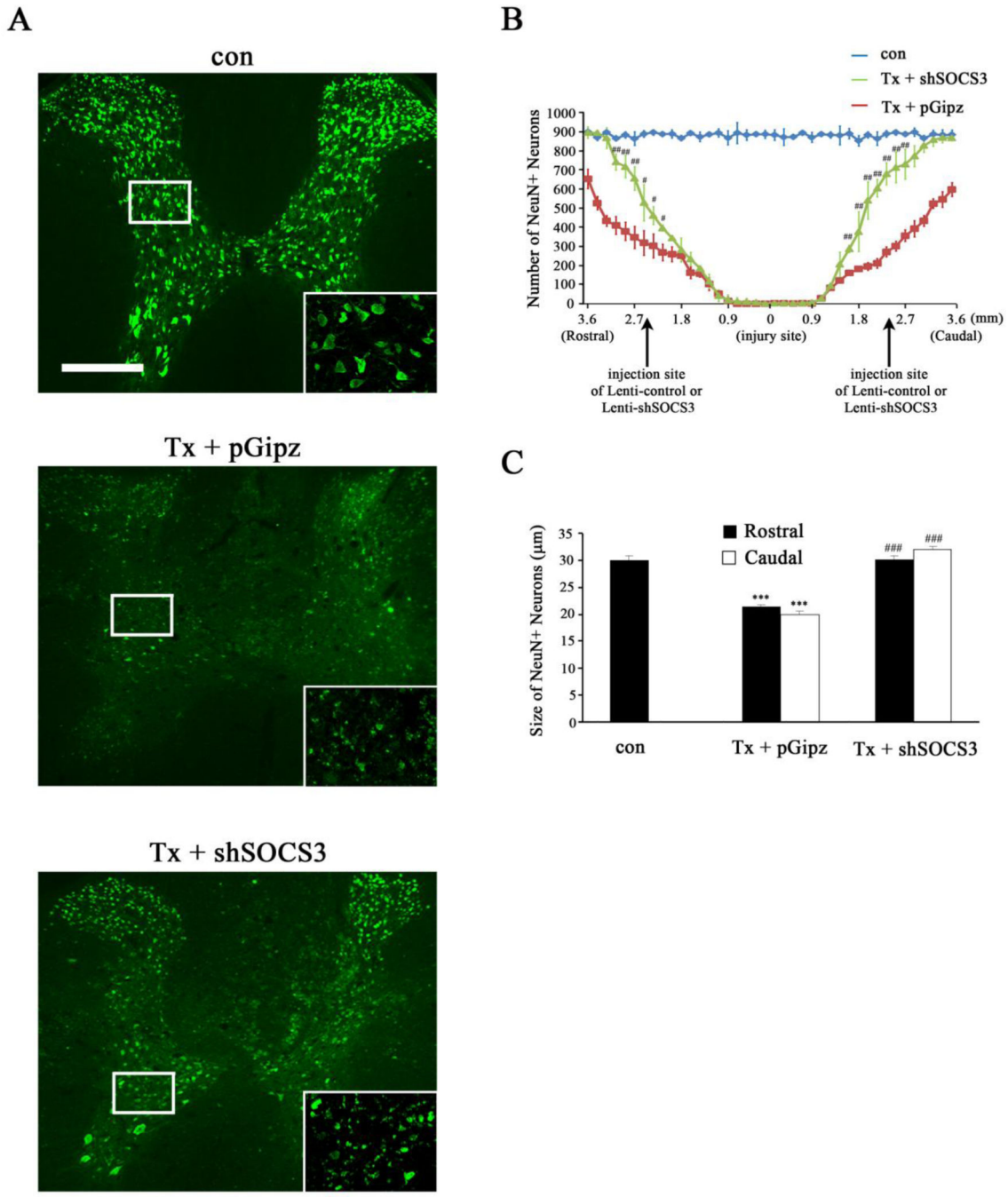

Figure 6. Reduction of SOCS3 expression by shSOCS3 contributed to neuroprotective effects after SCI

A, Representative images of a spinal cord transverse section (rostral to the injured site) from sham (con), pGipz-treated or shSOCS3-treated animals indicate that shSOCS3 significantly prevented NeuN+ neuronal cell death 7 days after SCI (Tx). The insets show higher magnifications of the NeuN+ neuronal population. Scale bar, 250 μm. **B**, Statistical analysis indicated the number of NeuN+ neurons in shSOCS3-treated animals was significantly higher than that in the pGipz-treated group 7 days after SCI in areas both rostral and caudal

to the injured site. #p < 0.05, ##p < 0.01, and ###p < 0.001 compared to pGipz treatment (ANOVA and Student-Newman-Keuls analyses). **C**, Statistical analysis indicated that the size of NeuN+ neurons with shSOCS3 treatment was significantly larger than those with pGipz treatment 7 days after SCI in areas both rostral and caudal to the injured site. ***p < 0.001 compared to sham control, and ###p < 0.001 compared to pGipz treatment (ANOVA and Student-Newman-Keuls analyses).

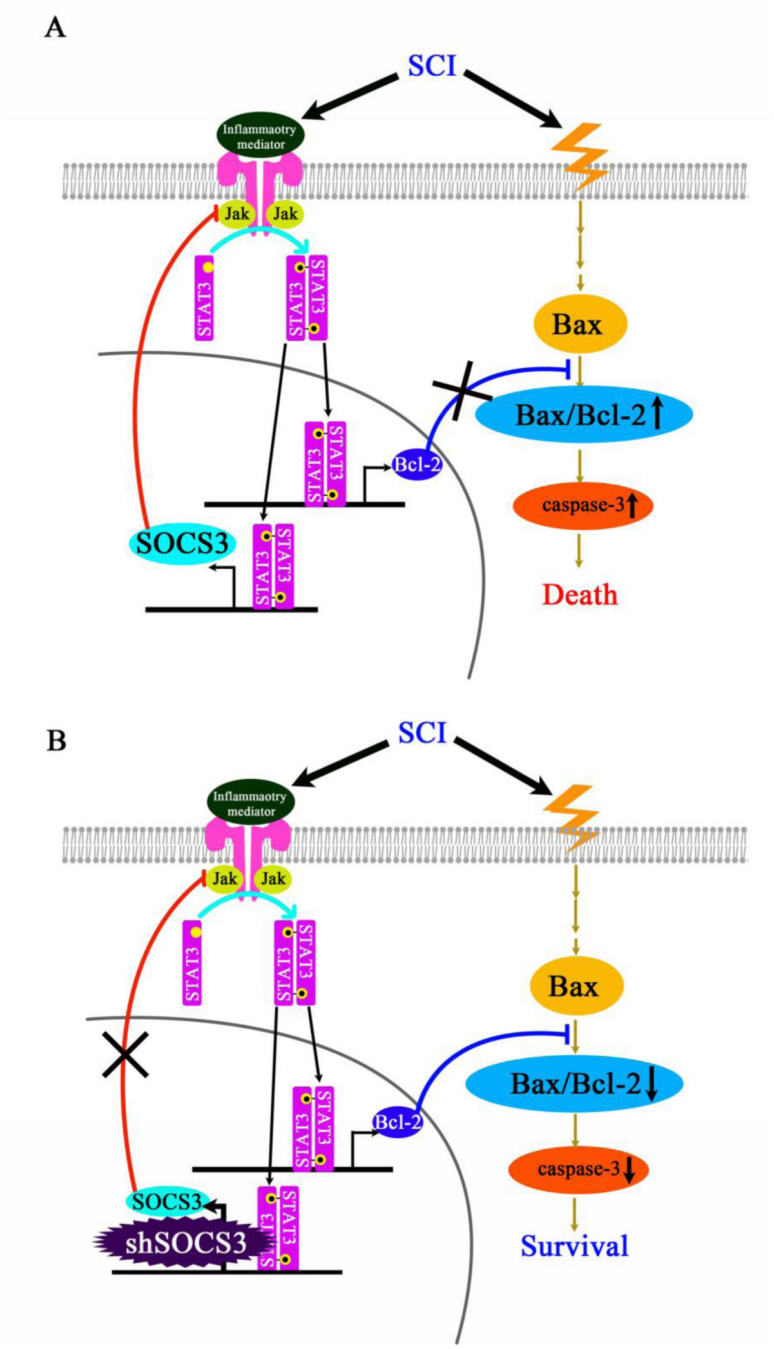

Figure 7. A proposed mechanism of how reduction of SOCS3 prevents neurons from SCI-induced cell death

A, SCI-induced increases in SOCS3 expression lead to inhibition of the Jak/STAT3 pathway, which in turn increases the Bax/Bcl-2 ratio. This contributes to SCI-induced neuronal death *in vivo*. **B**, Reduction of SOCS3 by shSOCS3 activates STAT3 signaling and decreases the Bax/Bcl-2 ratio, which consequently contributes to neuronal protection/ survival after SCI.